Paper Title: Enhancement of melting heat transfer of ice slurries by an injection flow in a rectangular cross sectional horizontal duct

Kota FUJII[*1], Masahiko YAMADA[*2, *3]

*1 Toyota Motor Corporation, Toyota-cho Toyota, Aich, 471-8572, Japan
*2 Division of Human Mechanical Systems and Design,
Graduate School of Engineering, Hokkaido University
N13-W8, Kita-ku, Sapporo, 060-8628, Japan
E-mail: myamada@eng.hokudai.ac.jp, Tel. & Fax: +81-11-706-6425
*3 Corresponding author

Abstract
Ice slurries are now commonly used as cold thermal storage materials, and have the potential to be applied to other engineering fields such as quenching metals to control properties, emergency cooling systems, and preservation of food and biomaterials at low temperatures. Although ice slurries have been widely utilized because of their high thermal storage densities, previous studies have revealed that the latent heat of ice particles is not completely released on melting because of insufficient contact between the ice particles and a heated surface. In this study, an injection flow that was bifurcated from the main flow of an ice slurry was employed to promote melting heat transfer of ice particles on a horizontal heated surface. The effects of injection angle and injection flow rate on local heat transfer coefficients and heat transfer coefficient ratios were determined experimentally. The results show that from two to three times higher heat transfer coefficients can be obtained by using large injection flow rates and injection angles. However, low injection angles improved the utilization rate of the latent heat of ice near the injection point by approximately a factor of two compared to that without injection.

Keywords: Ice slurry, Latent heat, Two-phase flow, injection flow, Melting heat transfer

Highlights

- Melting of ice slurries were enhanced by the injection under constant total flow rate.
- Contribution of ice particles and their latent heat to heat transfer was investigated.
- Effect of velocity ratio of injection to that of main flow was examined.
- Effect of the angle of injection flow to the main flow was also examined.
- Appropriate conditions for the use of latent heat of ice and heat transfer did not coincide.

ATE-2013-3782
Revised manuscript

Enhancement of melting heat transfer of ice slurries by an injection flow in a rectangular cross sectional horizontal duct

Kota FUJII[*1], Masahiko YAMADA[*2, *3]

*1 Toyota Motor Corporation, Toyota-cho Toyota, Aich, 471-8572, Japan

*2 Division of Human Mechanical Systems and Design,

Graduate School of Engineering, Hokkaido University

N13-W8, Kita-ku, Sapporo, 060-8628, Japan

*3 Corresponding author

E-mail: myamada@eng.hokudai.ac.jp, Tel. & Fax: +81-11-706-6425

Abstract

Ice slurries are now commonly used as cold thermal storage materials, and have the potential to be applied to other engineering fields such as quenching metals to control properties, emergency cooling systems, and preservation of food and biomaterials at low temperatures. Although ice slurries have been widely utilized because of their high thermal storage densities, previous studies have revealed that the latent heat of ice particles is not completely released on melting because of insufficient contact between the ice particles and a heated surface. In this study, an injection flow that was bifurcated from the main flow of an ice slurry was employed to promote melting heat transfer of ice particles on a horizontal heated surface. The effects of injection angle and injection flow rate on local heat transfer coefficients and heat transfer coefficient ratios were determined experimentally. The results show that from two to three times higher heat transfer coefficients can be obtained by using large injection flow rates and injection angles. However, low injection angles improved the utilization rate of the latent heat of ice near the injection point by approximately a factor of two compared to that without injection.

Keywords: Ice slurry, Latent heat, Two-phase flow, Injection flow, Melting heat transfer

1. Introduction

Since prehistoric times when human survival was based on hunting and agriculture, some forms of thermal storage technology has been recognized as important. Initially, people used controlled fires for heating and cooking by heating some type of stones. They sometimes used a cave to store snow or ice and preserve food at low temperatures.

Nowadays, heating and air-conditioning systems are widely used throughout the world. Nevertheless, thermal storage by latent heat for both high- and low-temperature applications is still being utilized and studied to save energy and reduce environmental problems.

Alternative sources such as solar energy and wind power offer large amounts of energy but at low energy densities. Therefore, it is natural to consider combining thermal storage systems with alternative energy sources. For example, in high-temperature systems, solar energy can be stored as the latent heat of a thermal storage material. The stored energy can then be used as the heat source of a heat pump system [1-3]. Similarly, in wind-power generation, excess electrical power can be used to heat stone bricks, thereby storing the excess energy as sensible heat.

In contrast, for low-temperature systems, ice and snow have long been used as thermal storage media. With the development of refrigeration systems, cold thermal

storage systems are sometimes combined with refrigerators to improve the performance of the cooling system and save electrical energy.

An ice-slurry, a mixture of ice particles and water or an aqueous solution, is often used as a thermal storage material in the cold thermal storage systems. It has many liquid-like properties, as well as the latent heat of ice particles is high. Depending on the weight ratio of ice to water, a slurry can have a latent heat that is larger than the sensible heat of the liquid alone. Furthermore, unlike an ice block, the melting heat transfer of a slurry can be substantially enhanced by convection and contact between the slurry and a heated surface. Ice slurries could be utilized for rapid cooling with high heat flux because of its high heat capacity due to its latent heat and direct contact heat transfer between ice particles and a heated surface. For example, ice slurries could be used in the emergency cooling systems of nuclear reactors to control the properties of materials by thermal treatments such as quenching, in the production of amorphous solids, and in the preservations of food and biomaterials at low temperatures. Moreover, in the storage and transport of liquefied gases, the mixed condition of liquid and solid of the gas, namely the slurry condition of the gaseous material, is advantageous because the melting latent heat of the solid absorbs any heat input, thereby preventing sudden volume changes.

In all the above-mentioned applications of ice slurries, the promotion of heat transfer on heated surfaces is essential. In other words, identifying effective ways to retrieve the latent heat from the phase change of solids in the slurries is necessary.

In conventional dynamic cold thermal storage systems using ice slurries, ice particles usually melt in a storage tank and their latent heat of melting is released through the ambient liquid. However, the latent heat melting ice is likely to be utilized more efficiently if ice particles melt on a heat transfer surface through direct contact.

The basic properties and melting heat transfer characteristics of ice-slurries for use in direct contact heat exchangers have been investigated previously. The critical review by Egolf and Kauffeld [4] and references therein show many previous studies of ice-slurry cold thermal storage systems; the properties studied include velocity profiles, ice-fraction profiles, pressure losses, and heat transfer rates for a variety of flow conditions. After the review by Egolf and Kauffeld, some studies have reported the melting heat transfer of ice-slurry flows through tubes, and correlation equations for melting heat transfer were derived from the results [5-8]. In addition, some numerical approaches have been exploited to build a heat transfer model for melting of ice slurries [9, 10].

In addition to the basic studies cited above, use of ice slurries as a secondary coolant

in heat exchangers has been widely investigated [11-13]. Kawanami et al. [14] reported that the latent heat of melting ice is not completely utilized within the heat transfer section having a heated surface. They measured ice fractions at both the inlet and outlet of a 1-m long horizontal flow duct with a horizontal heated surface at its bottom. They found only a small difference in ice fractions between the inlet and outlet. The melting rate of ice particles in a slurry was small probably because of the following reasons:

1) Depending on the configuration of the heat exchanger, maintaining direct contact between ice particles and the heated surface may be difficult.

2) A melted liquid film, which forms on the heated surface, serves as a boundary layer that prevents direct contact with ice particles.

At present, the advantage of high latent heat of ice particles may be irrelevant for using ice slurries. However, if the melting heat transfer of ice in the slurry can be enhanced, then a more efficient heat exchange in retrieving cold thermal energy could be achieved. This means that the size of the heat exchanger can be reduced. In addition, the use of ice slurries in emergency cooling systems of nuclear reactors could be realized.

The main idea of the present study is that the contribution of the latent heat of melting to heat transfer can be enhanced by making ice particles in the slurry directly

collide with the heated surface. Direct injection of the slurry onto a heated surface effects heat transfer in the following two ways: one is stated above and the other is the turbulent flow promotion, which will increase heat transfer.

The objectives of the present study are to determine the effects of a variety of conditions on local heat transfer characteristics and evaluate the contribution of the latent heat of melting ice to heat transfer when an injection system is employed.

Nomenclature

A_1 : cross-sectional area of main flow duct [m^2]

A_2 : cross-sectional area of injection flow duct [m^2]

C_d : drag coefficient

C_1 : initial concentration of aqueous solution [mass%]

C_2 : concentration of aqueous solution in ice slurry [mass%]

Fs : fraction of solid [wt%]

H : height of injection flow duct [m]

h_x : local heat transfer coefficient [W/m^2K]

Q_0 : total flow rate [m^3/s]

Q_1 : flow rate of main flow (at the inlet of duct) [m^3/s]

Q_2 : flow rate of injection flow [m^3/s]

q : heat flux at heated surface [W/m^2]

T_s : temperature of ice slurry at inlet of main flow duct [°C]

T_x : local temperature of heated surface [°C]

u_1 : mean velocity of main flow (in the duct before injection) [m/s]

u_2 : mean velocity of injection flow [m/s]

x : distance from the inlet of main flow duct [m]

(x, y) : coordinates in Eq. (5) and Fig. 3 [m]

Greek symbols

α : velocity ratio defined by Eq. (2)

δ : thickness of the two-dimensional jet at injection in Eq. (5)

η : heat transfer coefficient ratio defined by Eq. (4)

θ : angle between the flow axis of main flow and injection flow [deg.]

Subscripts

liq : single phase

s : ice slurry

ave : averaged

2. Experimental Apparatus and Method

2.1 Experimental apparatus

Figure 1(a) shows a schematic diagram of the experimental apparatus used in the present study. The apparatus mainly consists of a cooling brine circulation loop, an ice-slurry tank where ice slurry was produced and stored, an ice-slurry circulation loop including the test section, and measurement facilities.

The ice-slurry tank, whose capacity was 1.5 m^3, was made of an acrylic plate. It was separated into the following two parts: the area where the ice slurry was produced and a storage area. In the production area, a heat exchanger made of a silicone tube of 15-mm inner diameter was installed to produce the ice slurry by freezing an aqueous solution of ethylene glycol.

From the initial concentration of the ethylene glycol solution and temperature of the ice slurry in the production process, the solid fraction of produced ice slurry can be determined. After the predetermined solid fraction of ice slurry was obtained, the ice slurry was driven by a pump; its total flow rate was set and measured by an electromagnetic flow meter. Manipulating the main and bifurcation valves sets the flow rates at both the inlet of the test section and injection flow duct.

A detail of the test section is depicted in Fig. 1(b). The test section was a horizontal flow duct made of acrylic plates with a square cross-section of 60 mm × 60 mm and a length of 900 mm. At the middle of the test section, an injection duct, 60-mm wide and 20-mm high, was connected to the top plate of the main flow duct. The injection angle could be set to one of three orientations, namely 15°, 30°, and 45° to the direction of the main flow.

The bottom of the main flow duct was a Bakelite plate with a stainless foil heater (10-μm thick) on the surface. By setting the power input to the heater, a uniform heat flux could be achieved. Between the heater and base plate, twelve type-K thermocouples (ϕ = 300 μm) were installed to measure local temperatures on the heated surface. Four thermocouples were also placed at the inlet and outlet of the test section. The positions of the thermocouples are indicated in Fig. 1(b). The surface of the heater was electrically insulated by a coating spray.

2.2 Method

To produce ice slurries, an aqueous solution of ethylene glycol with initial concentration C_1 was cooled and frozen while being circulated. By assuming local equilibrium of concentration and temperature, C_2 was appropriately determined from

the temperature of the slurry. Then, the solid fraction of ice in the slurry *F*s could be calculated as

$$Fs = \left(1 - C_1/C_2\right) \times 100 \qquad [wt\%] \tag{1}$$

In the experiment, the pumped ice slurry was divided into the main flow (flow rate Q_1) and injection flow (flow rate Q_2). The total flow rate Q_0 (= Q_1 + Q_2) was maintained constant by controlling the main control and bifurcation valves. From each cross-sectional area A_1 and A_2 and flow rate Q_1 and Q_2, the mean velocities u_1 and u_2 can be determined. Then the velocity ratio α can be defined as

$$\alpha = u_1/u_2 \tag{2}$$

The heat flux of the heated surface q was maintained constant at 4000 W/m^2. This value was chosen from previous experimental results, which showed that the heat flux did not largely effect the heat transfer coefficient for the same order of heat flux and for the range of heat flux of the heat exchanger used in air-conditioning. The solid fraction was set at 0, 10, and 20 wt%. The injection angle to the main flow θ was set at 15°, 30°, and 45°. The total flow rate Q_0 was set at 0.72 × 10^{-3}, 1.44 × 10^{-3}, 2.16 × 10^{-3}, and 2.88 × 10^{-3} m^3/s. The flow velocity ratio α was set at 1, 3, and 9.

After steady state was achieved for each test condition, the distributions of local temperature at the heated surface were measured to determine the local heat transfer

coefficient h_x from

$$h_x = q/(T_x - T_s) \quad (3).$$

To evaluate the contribution of the latent heat of melting ice to the heat transfer coefficient, we introduced the heat transfer coefficient ratio η, which is expressed as follows:

$$\eta = h_{x,s}/h_{x,liq} \quad (4).$$

where $h_{x,s}$ is the local heat transfer coefficient for an ice-slurry flow and $h_{x,liq}$ is the local heat transfer coefficient of a single-phase flow (in this case, the ethylene glycol solution) with an injection flow. The heat transfer coefficient ratio η can be regarded as the contribution of the latent heat of melting ice to the overall local heat transfer coefficient.

2.3 Estimation of measurement errors

Errors in the measured data were estimated from the precision of instruments and fundamental measurements. For concentrations, errors were estimated to be 5% on the basis of the precision of the concentration meter. The precision of the flow velocity meter was 0.1% and that of the cross-sectional area was 2.5%; consequently, errors in volumetric flow rates were estimated to be 2.6%. In the same way, errors in the heat

transfer coefficients from Eq. (3) were estimated to be 3.6% on the basis of the precisions of voltage, electric current, surface area, and temperature measurements. The time average of the measured data during the minute after achieving steady state was employed in calculating the results (120 data points sampled every 0.5 s).

3. Results and Discussion

The injection flow was appropriately bifurcated from the main flow while keeping the total flow rate constant. The injection point was at the middle of the test section. Therefore, heat transfer before the injection point was readily predicted to decrease because of the decrease in flow rate due to the bifurcation, in contrast to the increase in heat transfer resulting from the injection. The present investigation aims to determine the optimum conditions for the bifurcated injection flow, such as its flow rate and injection angle.

3.1 Enhancement of local heat transfer of the single-phase flow by injection

The effect of injection without ice particles was determined using a single-phase fluid (the ethylene glycol solution). Figure 2 shows the local heat transfer coefficients for a various velocity ratios and injection angles under constant heat flux. The local heat

transfer coefficients on a horizontal heated plate with constant heat flux, which were derived from approximate solutions of boundary layer equations by employing the von Kármán integral expression [15], are indicated by the bold solid line in this figure.

In the area upstream of the injection, experimental values are slightly higher than those predicted theoretically because the theoretical values are derived for a semi-infinite plate; though, in the duct flow of the present study, the liquid temperature increases along the flow, thereby reducing the temperature differences. Another reason is the effect of swirl formed by the injection flow. These effects are discussed below. Figure 2 clearly shows that local heat transfer coefficients before injection depend mainly on α that determines the velocity of the main flow; in contrast, the heat transfer coefficients are almost independent of θ.

In the area downstream of the injection, local heat transfer depends on both α and θ. As shown in Fig. 2, both larger injection velocities and angles increase the local heat transfer coefficients by approximately three times than those obtained theoretically. At x = 500 mm, local heat transfer shows a maximum at $\alpha = 9$ and $\theta = 45°$.

Abramovich [16] used a theoretical approach to propose an equation that predicts a flow axis for a two-dimensional jet into a horizontal flow.

$$\frac{y}{\delta}\frac{C_d}{\alpha^2} = 2\sin\theta\left(\sqrt{C_d\frac{x}{\delta}\frac{1}{\alpha^2}\frac{1}{\sin\theta}+\cot^2\theta}-\cot\theta\right) \quad (5)$$

Note that Eq. (5) was originally derived for a single-phase case under a semi-infinite field. Figure 3 shows the flow axes of the injection flow under a variety of velocity ratios and injection angles. The main flow runs horizontally from left to right and injection flow makes an angle θ, as shown in this figure.

In the present study, the injection flow impinges on a heated bottom wall, particularly at large inlet velocities and angles. The injected flow collides with and reflects the bottom wall, promoting the turbulent flow and consequently enhancing heat transfer.

At small velocity ratios (small injection velocities), the injection flow may not reach the bottom wall because of the effects of low inertia and main flow from the sides. In these cases, the injection flow will push the main flow down to the heated bottom surface. Therefore, heat transfer is still expected to be enhanced.

In contrast, at high injection velocities (α = 9), the injected flow will reach the bottom wall and interrupt the main flow. As a result, the main flow forms swirls just before the injection area, increasing heat transfer at the point. These phenomena play an important role to characterize local heat transfer on the bottom wall near and after the injection point. In the case of the ice-slurry flow, flow characteristics around the

injection flow are expected to exert even stronger effects on heat transfer.

3.2 Heat transfer enhancement of the ice-slurry flow by injection

3.2.1 Effect of solid fraction and injection angle

Figure 4 shows the effect of solid fraction on the local heat transfer coefficients for different injection angles. The solid fraction of ice slurry *F*s varied from 0 (single phase) to 20 wt%. Other factors such as total flow rate Q_0 and α were maintained constant, as shown in this figure.

In the area before injection, h_x is small because the main flow velocity is the smallest in the experiment (α = 9). The local heat transfer coefficients h_x show small differences for all cases of θ and *F*s.

However, just after the injection point ($x \approx 500$ mm), local heat transfer coefficients suddenly increase for $\theta = 45°$ at every *F*s condition. In addition, the cases of *F*s = 20 wt% ($\theta = 30°$ and 15°) also show large increases in h_x. The differences in heat transfer coefficient for the cases with *F*s = 10 wt% compared to those for the single- phase case are small. Thus, for all conditions in Figure 4, h_x abruptly increases just after the injection point. These results indicate that h_x is higher at larger solid fractions and inlet angles.

The heat transfer coefficient ratio η, which is defined in Eq. (4), is shown in Fig. 5, for the same conditions as those in Fig. 4. At θ = 45° and *Fs* = 20 wt%, where h_x is highest, the heat transfer coefficient ratio η is small. However, η is highest near the injection point at *Fs* = 20wt% with θ = 15° and 30°.

3.2.2 Effect of velocity ratio and injection angle

Figure 6 shows the effect of velocity ratio on the local heat transfer coefficients. The local heat transfer coefficients before the injection point seem to be almost independent of θ and are affected only by α, namely by the flow rate. After the injection point (x = 450 mm), both α and θ dominate the flow condition at and after the injection point; therefore, the heat transfer characteristics such as melting behavior improve.

Figure 7 shows the heat transfer coefficient ratio η for conditions corresponding to those in Fig. 6. By combining with the results shown in Fig. 5, particularly for the case of α = 9, the highest value of η is approximately 1.9 around the injection point for θ = 15° and 30°. However, for θ = 45°, η decreases to 1.3. This suggests that contributions of the latent heat of the ice-slurry decrease with increases in the injection angle. In the region x = 700 - 800, an increase in η occurs for α =3 and θ = 15°. This increase could be caused by the turbulence formed by the main and injection flows.

3.2.3 Effect of total flow rate and injection angle

In the area before injection, local heat transfer coefficients h_x may strongly depend on the total flow rate at constant Fs and α. As previously stated in the discussion of Fig. 3, the injection flow will push down or block the main flow, depending on α. Then, the reflection or swirls formed before the injection flow will affect h_x just before the injection area, as shown in Fig. 8. The local heat transfer coefficients after the injection show a tendency to increase with the total flow rate.

Because of the mechanism previously described, for θ = 45°, h_x showed its maximum and the differences in h_x caused by the flow rate are rather small. However, for θ = 30°, the area where h_x show its maximum shifts in the downstream direction. For θ = 15°, the effect of increasing the flow rate is clearly observed.

Figure 9 shows the heat transfer coefficient ratios for a variety of total flow rates and injection angles. The heat transfer coefficient ratio shows a steep increase at the injection point for θ = 15°. For θ = 30°, η takes its highest value just after the injection point. For θ = 45°, η does not increase very much. For larger injection angles, though the effect of injection on the heat transfer coefficient is large, the effect of the latent heat of ice particles on the local heat transfer is not as large as expected.

3.3 Overall evaluation

In the above discussions for the Figs. 4 - 9, the effects of parameters on h_x and η were discussed. While the behaviors of h_x and η seem to be clear, separating the effects of individual parameters is rather difficult. Integrated averages of both h_x and η were employed to evaluate behavior in the following three areas: before the injection area, after the injection area, and on the total area of the heated surface. For each area, the effects of α and θ were discussed.

Figure 10 shows the average of the local heat transfer coefficients $(h_x)_{ave}$. Note that an "average local heat transfer coefficient" differs from an "average heat transfer coefficient."

In general, in the case of the horizontal heated plate, h_x is highest at the inlet and gradually decreases along the flow, as shown in Fig. 2. Both the injection velocity and injection angle dominate the "average local heat transfer coefficient" $(h_x)_{ave}$ in the area after injection. As shown in Fig. 10, in the present results, $(h_x)_{ave}$ in the area after injection is highest for $\alpha = 9$ and $\theta = 45°$. However, the values averaged over the total area are clearly almost independent of injection angle, while they decreased at $\alpha = 3$ for every θ and showed the smallest values at $\alpha = 3$ and $\theta = 30°$.

Figure 11 shows the average of the heat transfer coefficient ratios η_{ave}. For $\theta = 15°$,

values of η_{ave} over the total area are a little higher than those for the single-phase solution ($\eta_{ave} > 1$) because of the effect of the latent heat of ice in the slurry. For $\theta =$ 30° and $\alpha = 9.0$, η_{ave} shows its maximum value ($\eta_{ave} = 1.3$) in the present results.

Now let us compare Figs. 10 and 11. Although the highest "average local heat transfer coefficient" $(h_x)_{ave}$ for the total area was obtained for $\alpha = 9$ and $\theta = 45°$, the cases for $\theta = 15°$ provide much better values of η_{ave} over the total area. If we carefully observe Fig. 10 for the case $\theta = 15°$, then we notice that higher results for $(h_x)_{ave}$ are consistently obtained. The mechanism of these tendencies can be explained with reference to Fig. 12. For small injection angles, the injection flow will push ice particles in the main flow to the heated surface, as shown in the figure. As a result, contact between ice particles and the heated surface will be better than that in the other cases.

4. Conclusions

In the present study, we investigated an injection method for enhancing the melting heat transfer of ice slurries. In our method, which differs from the conventional injection method, the ice-slurry flow was bifurcated before the heat transfer section into two flow lines: the main flow and injection flow into the heat transfer section. One advantage of this approach is that an additional pump is not needed to drive the

injection flow. However, when the total flow is maintained constant, an increase in the injection flow causes a decrease in the main flow rate; this causes a decrease in heat transfer by forced convection of the main flow. In the present study, experiments on the melting heat transfer of ice slurries were performed under conditions of constant heat flux at the horizontal heated surface that was a part of the heat transfer section.

Our experimental results for local heat transfer coefficients include the overall mechanism of heat transfer in a multiphase flow with a phase change. Furthermore, η measures the heat transfer enhancement produced by a solid-liquid two-phase flow compared to that produced by a single-phase flow; η also contains contributions of the latent heat of melting ice in the ice slurry.

Although we obtained different tendencies for the heat transfer coefficient and heat transfer coefficient ratio, evaluations using the heat transfer coefficient ratio η were thought to be more appropriate because large values of η imply heat transport mechanisms in which the latent heat of the ice slurry is efficiently utilized.

The injection flow not only enhances the heat transfer by ice particles colliding with the heated surface but also pushes the main flow down to the heated surface, at least for small values of α and θ. Therefore, even when the main flow rate is small, by setting α and θ appropriately, the enhanced heat transfer due to melting ice will be available.

We found that the most suitable conditions for utilizing the latent heat of ice slurries occur at relatively high solid fractions *Fs*, low flow rates of the main flow, and injection angles of 15° - 30°. Depending on the size and other conditions of the heated section, the most suitable injection point into the main flow, along with other conditions, may differ from the injection point used here.

The data obtained in the present study give appropriate conditions for enhancing the melting of ice particles. Our results provide basic data for designing a highly efficient heat exchanger between air and ice slurries, which could be applied to air-conditioning systems in large buildings and factories. In addition, the results obtained in the present study suggest possible applications of ice slurries to other problems, such as quenching of metals to control properties, emergency cooling systems, and preservation of food and biomaterials at low temperatures.

Acknowledgements

The authors would like to thank Enago (www.enago.jp) for the English language review.

References

[1] M. Esen, Thermal Performance of a Solar-Aided Latent Heat Store Used for Space Heating by Heat Pump, Solar Energy 69-1 (2000) 15-25.

[2] M. Esen, Aydin Durmus, Ayla Durmus, Geometric Design of Solar-Aided Latent Heat Store Depending on Various Parameters and Phase Change Materials, Solar Energy 62-1 (1998) 19-28.

[3] M. Esen, T. Ayhann, Development of a Model Compatible with Solar Assisted Cylindrical Energy Storage Tank and Variation of Stored Energy with Time for Different Phase Change Materials, Energy Convers. Mgmt. 37-12 (1996) 1775-1785.

[4] P. W. Egolf, M. Kauffeld, From physical properties of ice slurries to industrial ice slurry applications. Int. J. Refrig. 28 (2005) 4-12.

[5] M. Grozdek, R. Khodabandeh, P. Lundqvist, B. Palm, Å. Melinder, Experimental investigation of ice slurry heat transfer in horizontal tube, Int. J. Refrig. 32 (2009) 1310-1322.

[6] T. S. Evans, G. L. Quarini, G. S. F. Shire, Investigation into the transportation and melting of thick ice slurries in pipes, Int. J. Refrig. 31 (2008) 141-151.

[7] B. Niezgoda-Zelasko, J. Zelasko, Melting of ice slurry under forced convection conditions in tubes, Exper. Therm. and Fluid Sci. 32 (2008) 1597-1608.

[8] D. W. Lee, E. S. Yoon, M. C. Joo, A. Sharma, Heat transfer characteristics of the ice slurry at melting process in a tube flow, Int. J. Refrig. 29 (2006) 451-455.

[9] B. Niezgoda-Zelasko, Heat transfer of ice slurry flow in tubes, Int. J. Refrig. 29 (2006) 437-450.

[10] T. Kousksou, A. Jamil, Y. Zeraouli, J.-P. Dumas, DSC study and computer modelling of the melting process in ice slurry, Thermochemica Acta 448 (2006) 123-129.

[11] W. Lu, S. A. Tassou, Experimental study of the thermal characteristics of phase change slurries for active cooling, Applied Energy 91 (2012) 366–374.

[12] J.-P. Be´de´carrats, F. Strub, C. Peuvrel, Thermal and hydrodynamic considerations of ice slurry in heat exchangers, Int. J. Refrig. 32 (2009) 1791-1800.

[13] P. Pronk, C. A. Infante Ferreira, G. J. Witkamp, Superheating of ice slurry in melting heat exchangers, Int. J. Refrig. 31 (2008) 911-920.

[14] T. Kawanami, M. Yamada, M. Ikegawa, Flow and Heat transfer Characteristics of Ice Slurry in a Bending Flow Channel with Rectangular Cross Section, Trans. of JSME, Ser. B, 69-678 (2003) 422-429.

[15] R. B. Bird, W. E. Stewart, E. N. Lightfoot, Transport Phenomena, 2nd ed., J. Wiley & Sons Inc., New York, (2002) 136.

[16] G. N. Abramovich, Theory of Turbulent Jets, Translation published by MIT Press, Massachusetts (1963) 671.

Captions of Figures

Figure 1 a) Schematic diagram of experimental apparatus
b) Details of test section (main flow duct: inner dimensions 60 mm × 60 mm × 950 mm; injection flow duct: 60-mm wide and 20-mm high)

Figure 2 Local heat transfer coefficient of single phase flow with injection (effects of α and θ, $Q_0 = 0.72 \times 10^{-3}$ m^3, Fs = 20wt%, and q = 4000W/m^2)

Figure 3 Trace of injection flow core [12]

Figure 4 Local heat transfer coefficient (effects of Fs and θ, $Q_0 = 0.72 \times 10^{-3}$ m^3, $\alpha = 9.0$, and q = 4000 W/m^2)

Figure 5 Ratio of heat transfer coefficient of ice-slurry flow to that of single-phase flow (effects of Fs and θ, with injection flow, $Q_0 = 0.72 \times 10^{-3}$ m^3, $\alpha = 9.0$, and q = 4000 W/m^2)

Figure 6 Local heat transfer coefficient (effects of α and θ, $Q_0 = 0.72 \times 10^{-3}$ m^3, Fs = 20 wt%, and q = 4000 W/m^2)

Figure 7 Ratio of heat transfer coefficient of ice- slurry flow to that of single- phase flow (effects of α and θ, with injection flow, $Q_0 = 0.72 \times 10^{-3}$ m^3, Fs = 20 wt%, and q = 4000 W/m^2)

Figure 8 Local heat transfer coefficients (effect of Q_0, Fs = 20 wt%, α = 9.0, and q = 4000 W/m^2)

Figure 9 Ratio of heat transfer coefficient of ice-slurry flow to that of single-phase flow (effect of Q_0, with injection flow, Fs = 20 wt%, $\alpha = 9.0$, and q = 4000W/m^2)

Figure 10 Average of the local heat transfer coefficients

Figure 11 Average of the ratios of heat transfer coefficient of ice-slurry flow to that of single-phase flow

Figure 12 Flow image of ice slurry in the test section with injection

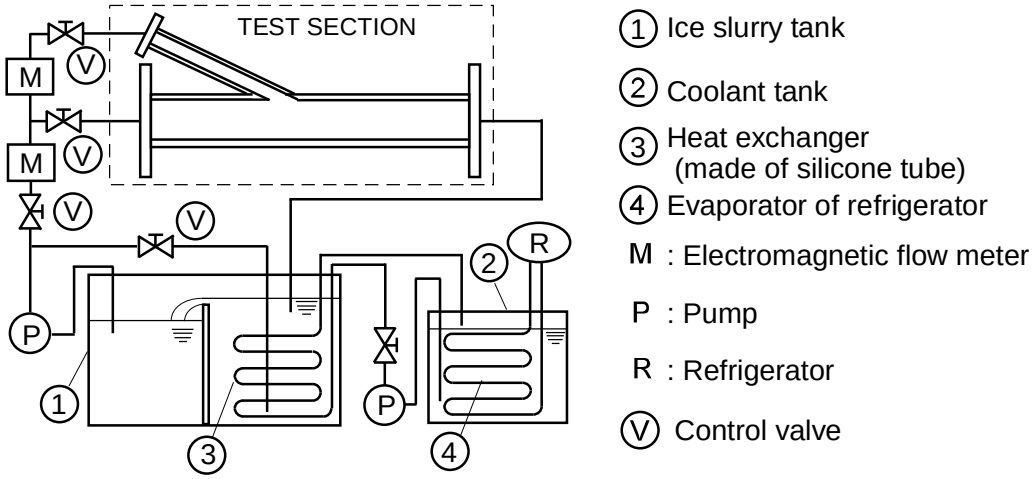

(a) Schematic diagram of experimental apparatus

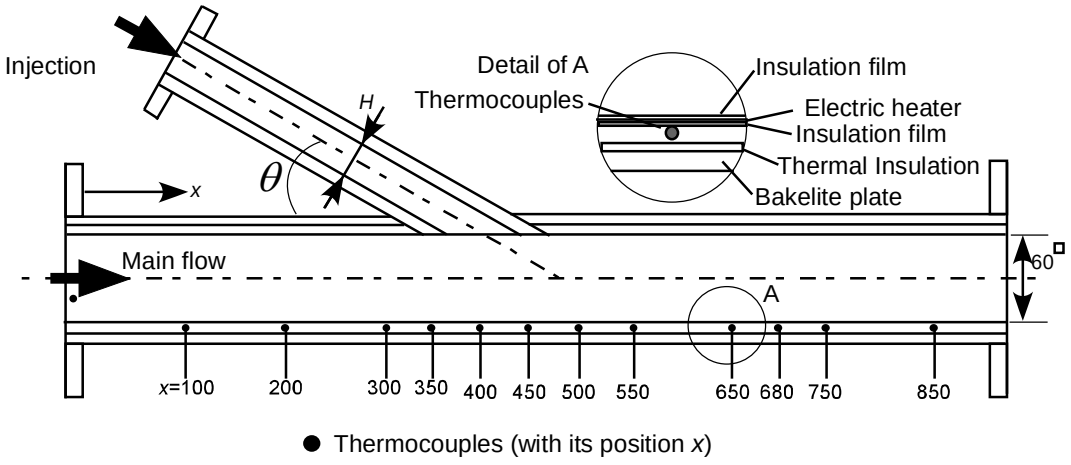

(b) Details of test section

Figure 1

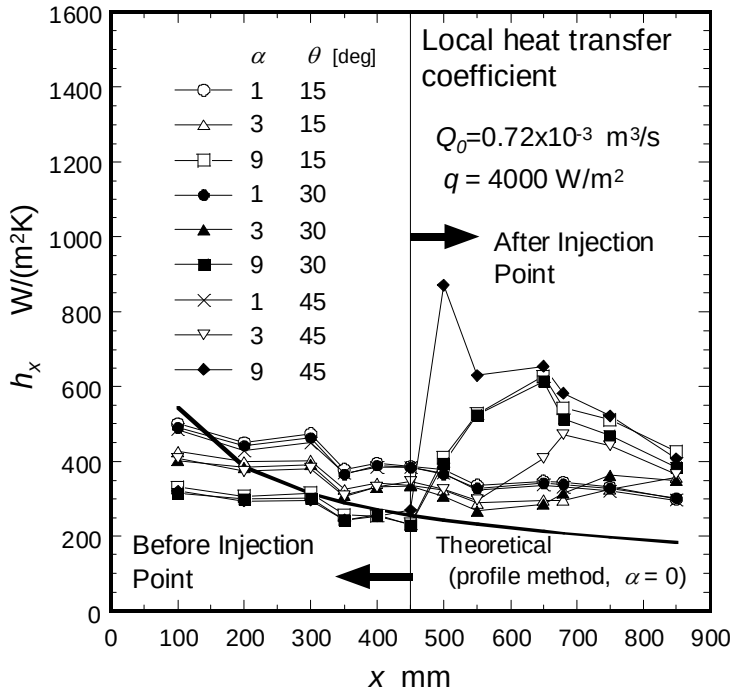

Figure 2

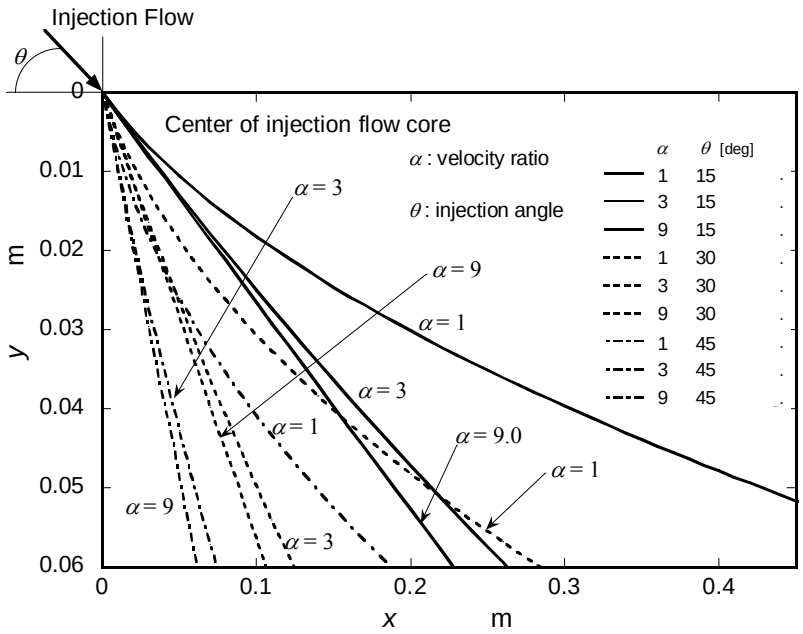

Figure 3

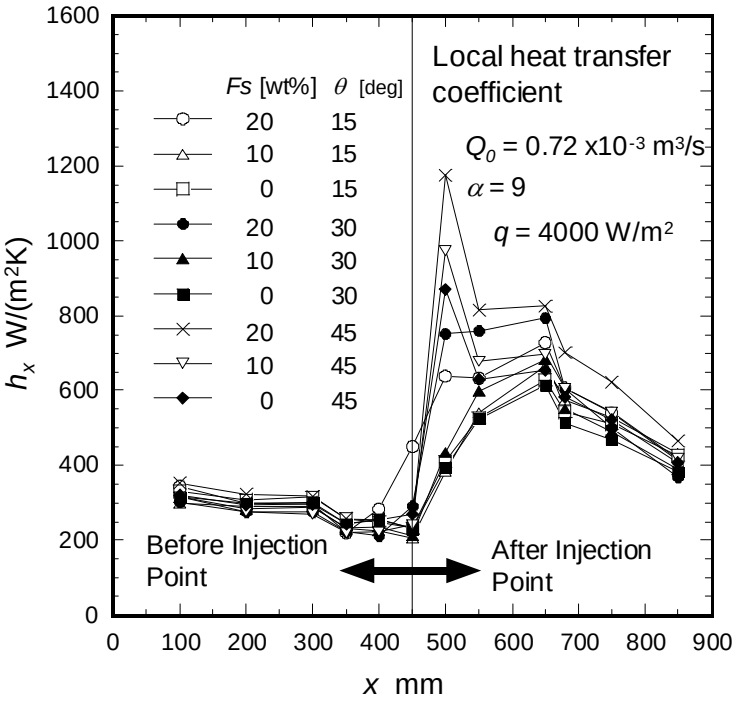

Figure 4

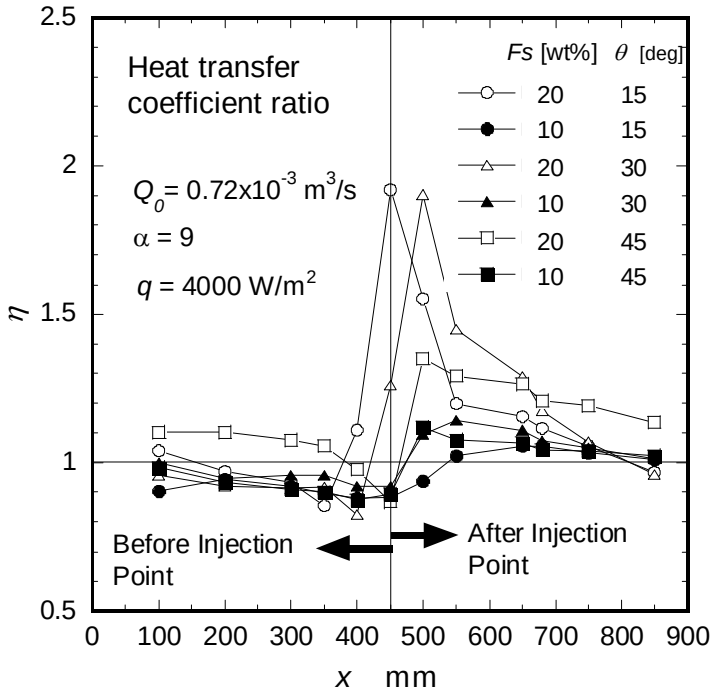

Figure 5

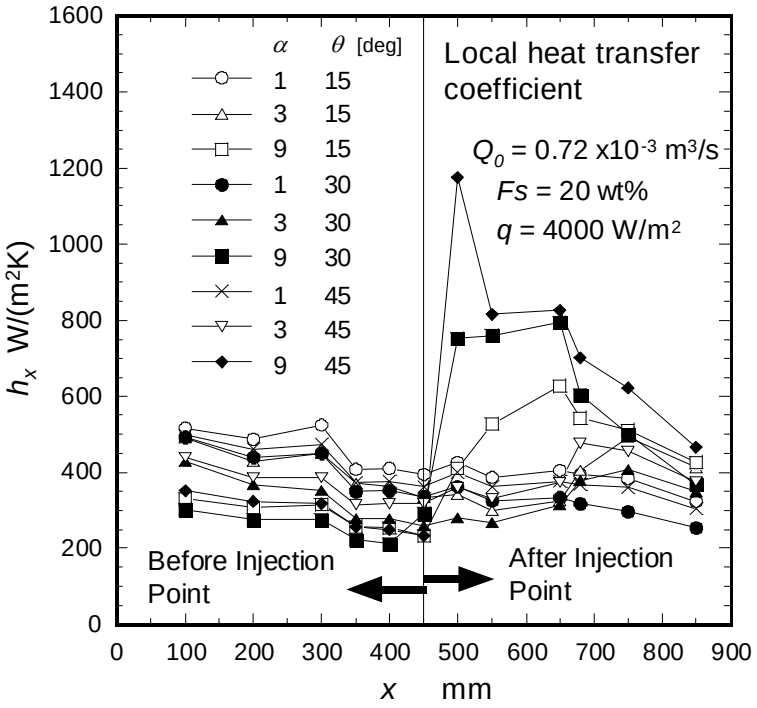

Figure 6

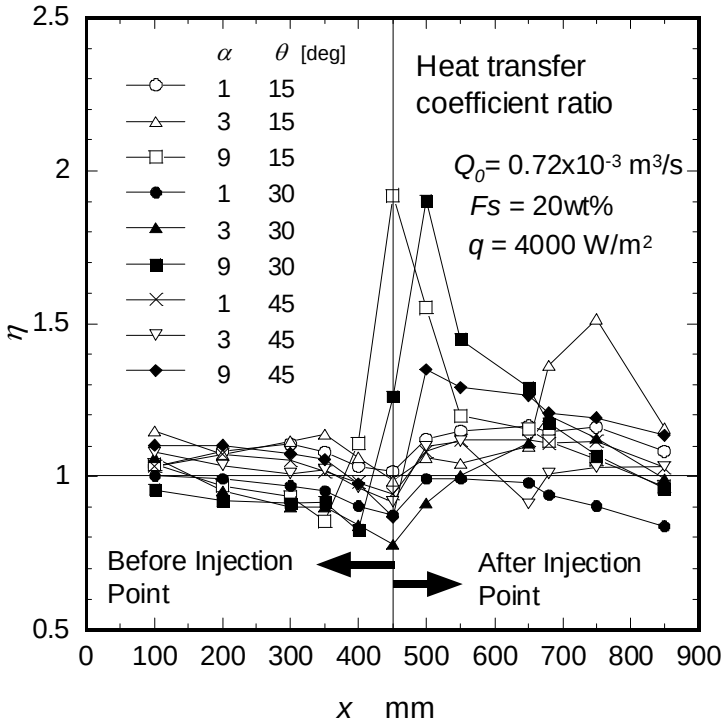

Figure 7

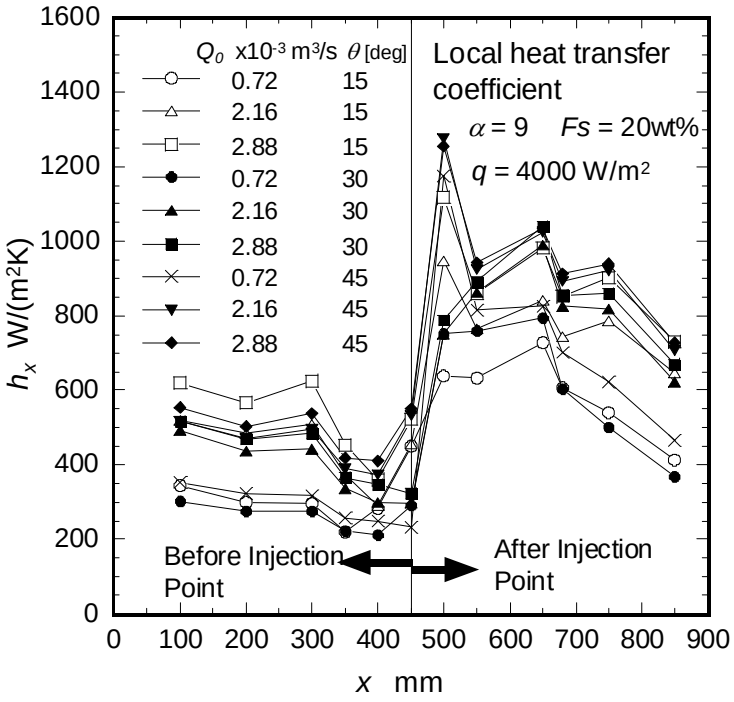

Figure 8

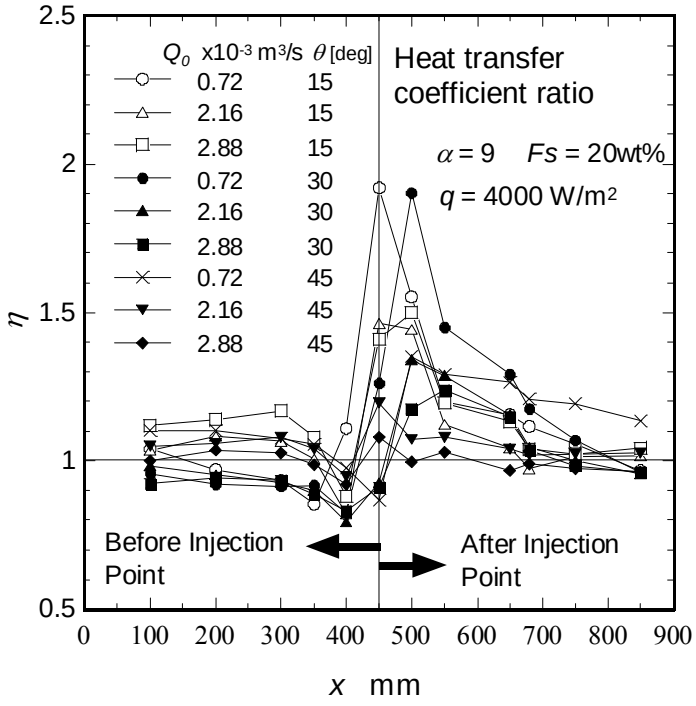

Figure 9

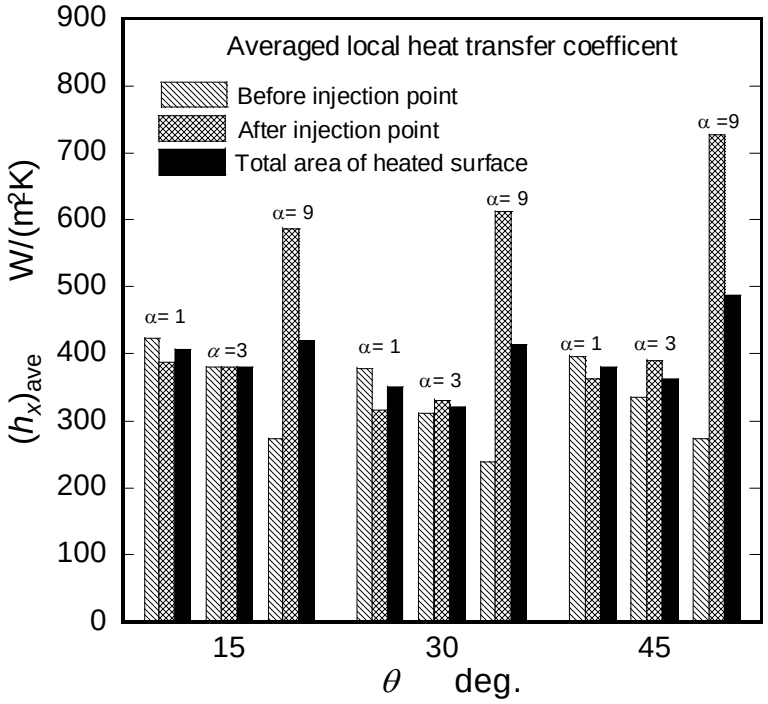

Figure 10

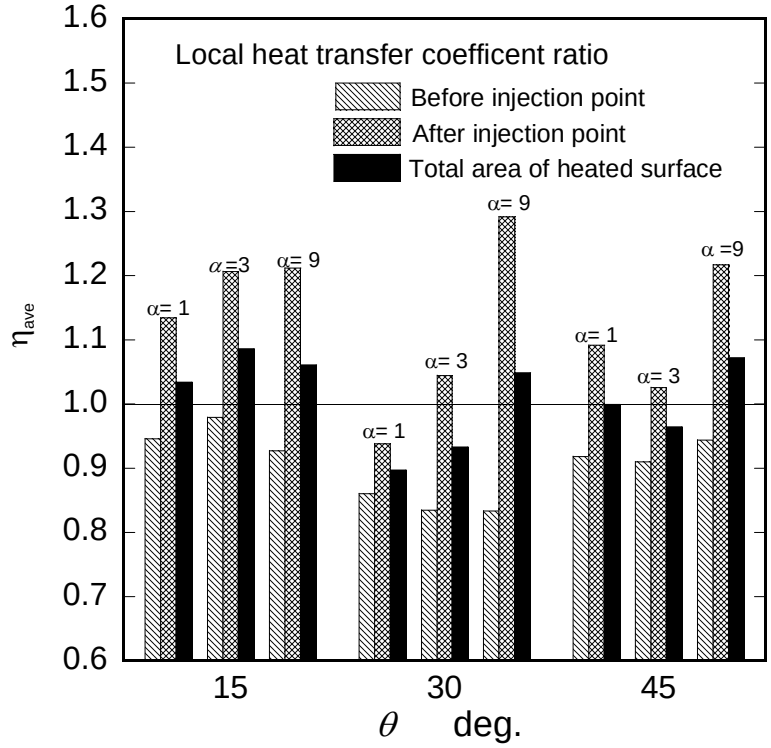

Figure 11

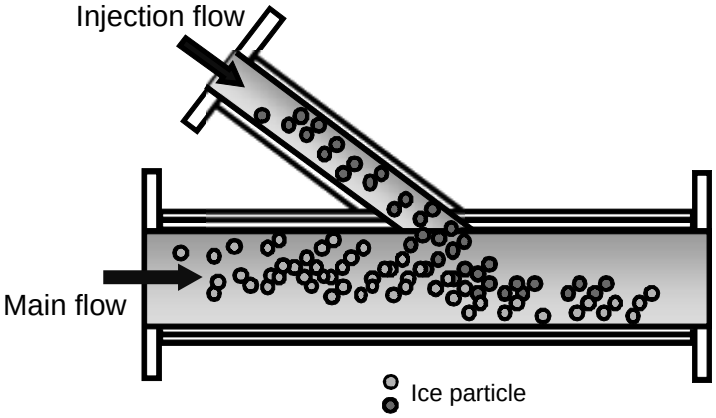

Figure 12